doi:10.1038/nature09819

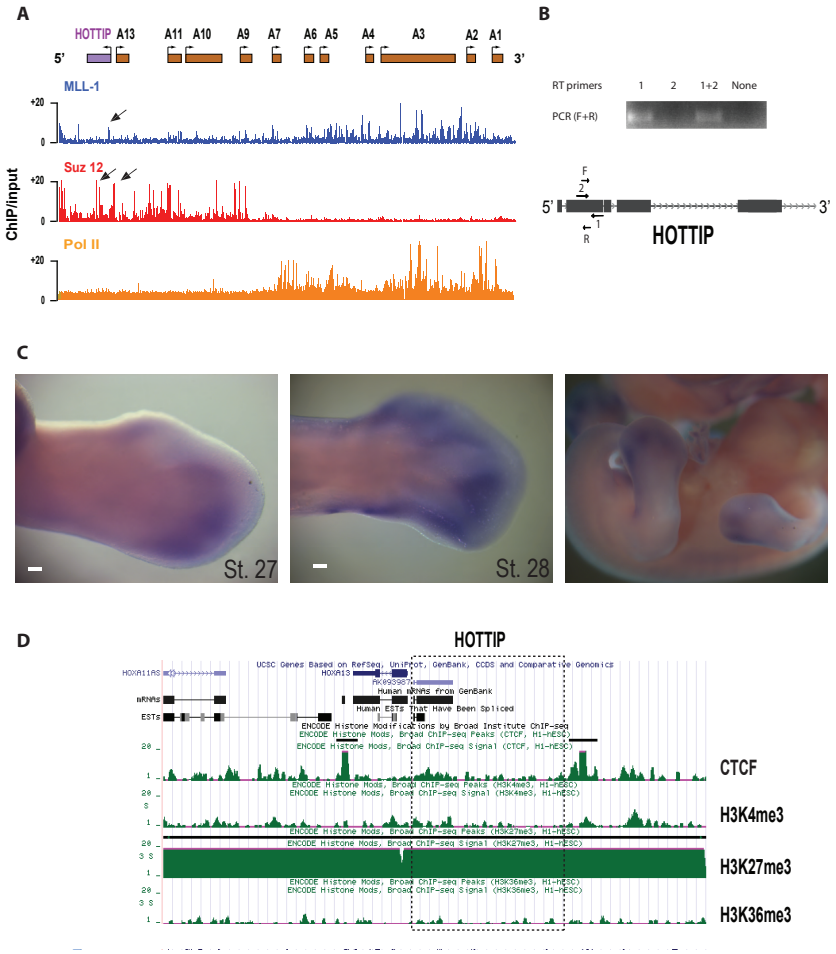


**Figure S1.** Molecular characterization of HOTTIP. (A) ChIP-chip confirmed that Suz12, a subunit of PRC2, and MLL1 both occupy *HOTTIP* in human lung fibroblasts, where HOTTIP RNA is not expressed. Chromatin occupancy map across the ~100 kilobase *HOXA* locus is shown. Genomic coordinate is on the X-axis; Y-axis depicts relative occupancy of MLL1, Suz12, and RNA polymerase II (Pol II) on a linear scale. Arrows depict MLL1 and Suz12 binding on *HOTTIP* DNA. Note that the peak of MLL1 occupancy coincides with diminished Suz12 binding, which are flanked by regions of higher Suz12 occupancy. This reciprocal binding of MLL and Polycomb subunits, even when both are present and juxtaposed, have been previously observed in bivalent domains[21]. (B) Strand-specific RT-PCR of HOTTIP RNA. Primer combinations used for reverse transcription (1, 2) and HOTTIP PCR (F, R) are diagrammed on the schematic. (C) Conserved distal expression pattern of chick HOTTIP. In situ hybridization of stage

28 chick embryo limbs are shown. White scale bar=0.1 mm. (D) Chromatin marks at the distal *HOXA* locus in human embryonic stem cells (ESC). In ES cells, the entire *HOX* loci, including *HOTTIP*, is marked by a broad domain of H3K27me3; the *HOTTIP* locus has no H3K4me3 or H3K36me3 marks, consistent with its silent status. Genome graphic data exported from http://genome.ucsc.edu/, utilizing the ENCODE whole genome data sets[22].

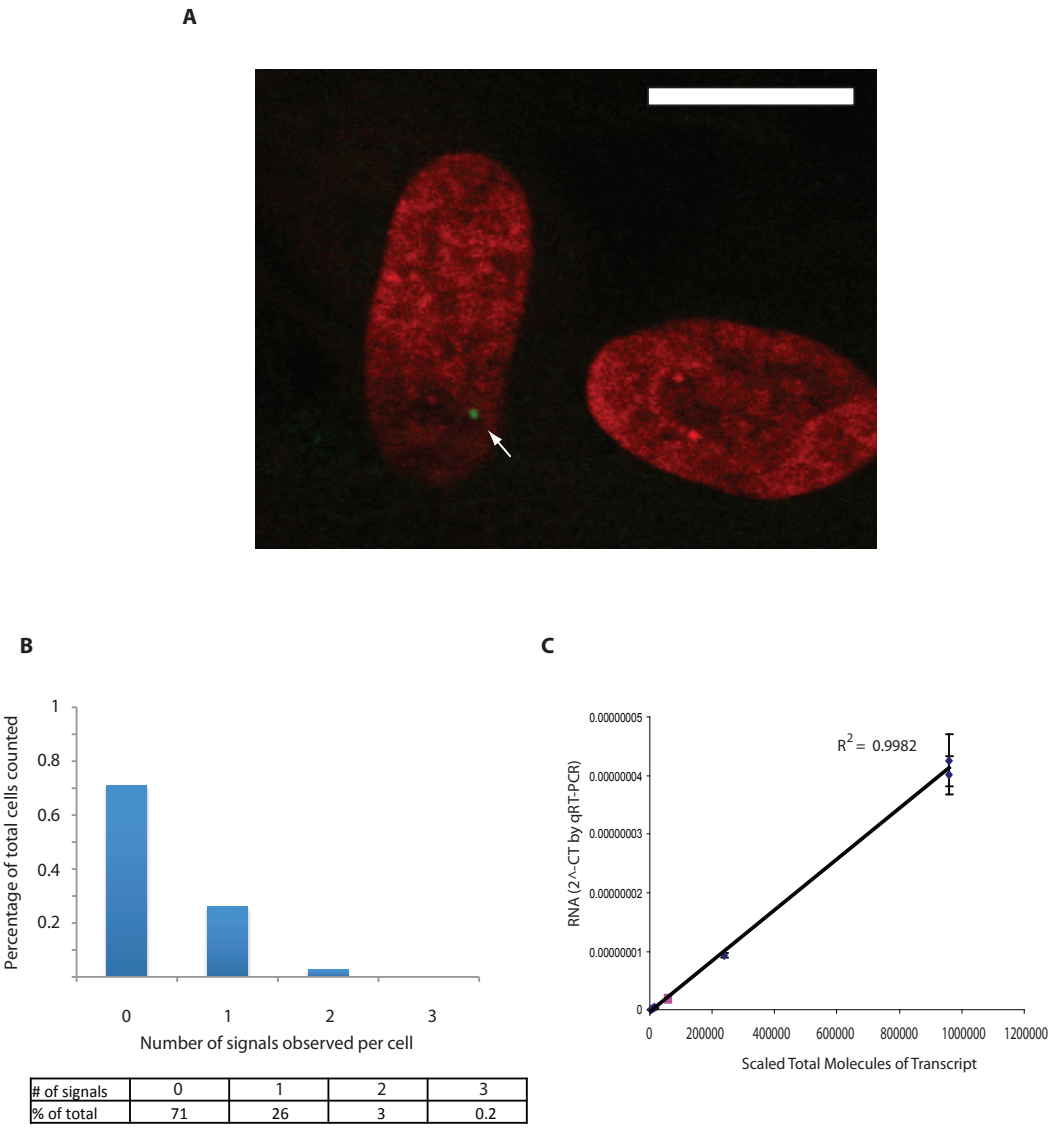


| # of signals | 0 | 1 | 2 | 3 |
|---|---|---|---|---|
| % of total | 71 | 26 | 3 | 0.2 |

**Figure S2.** Single molecule RNA-fluorescence *in situ* hybridization (FISH) confirms low copy number of HOTTIP RNA. (A) Primary human foreskin fibroblasts were hybridized with a mixture of Cy-5-labeled probes against HOTTIP and assayed for HOTTIP expression via confocal microscopy. Representative confocal images showing an example of a cell with one (left) or no (right) copies of HOTTIP RNA (green, highlighted

by arrow). DAPI staining of cellular nuclei is in red. White scale bar=15μm. (B) Quantitation of RNA-FISH experiments, demonstrating that the majority (>97%) of the cells examined contain zero or one copy of HOTTIP RNA. HOTTIP RNA is present on average at 0.31 copies per cell. The counts were pooled from 3 independent replicates (n=449 cells). (C) Titration curve used to determine number of HOTTIP molecules per 500,000 cells. Y-axis depicts 2^-ct values from qRT-PCR; X-axis depicts scaled total molecules of transcript in a sample. Blue points outline the titration curve using a known quantity of HOTTIP molecules to determine corresponding qRT-PCR 2^-ct values; error bars represent s.d. from three technical replicates. The pink square represents the qRT-PCR value from a standard sample of 500,000 foreskin fibroblasts.

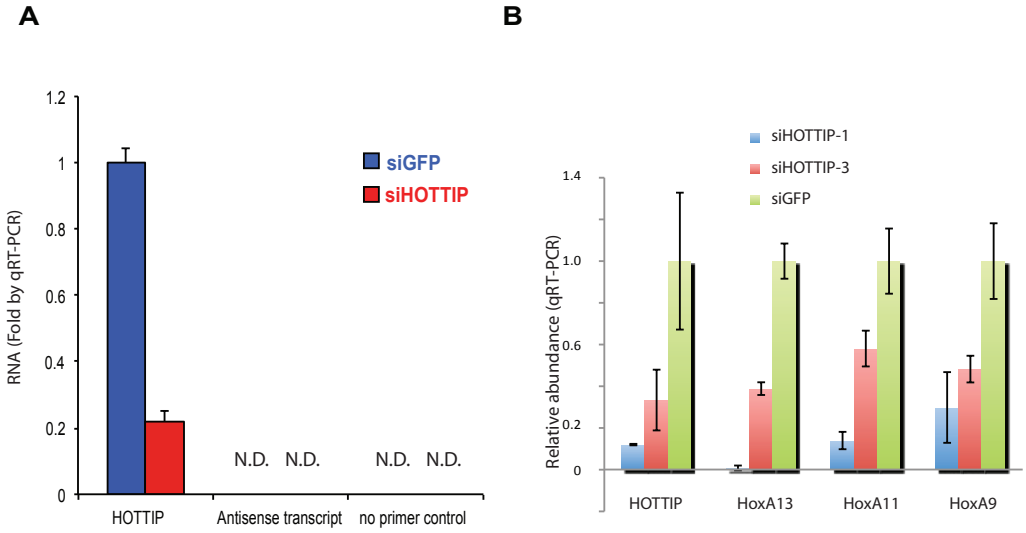


**Figure S3.** Lack of antisense HOTTIP RNA with HOTTIP knockdown. (A) No antisense transcription upon HOTTIP depletion. RNA from foreskin fibroblasts treated with control or HOTTIP siRNA was reverse transcribed with strand-specific primers, and then transcript abundance is analyzed by qPCR. N.D. not detectable. (B) Independent siRNAs targeting HOTTIP abrogated 5' *HOXA* gene expression in primary fibroblasts. Mean ± s.d. are shown.

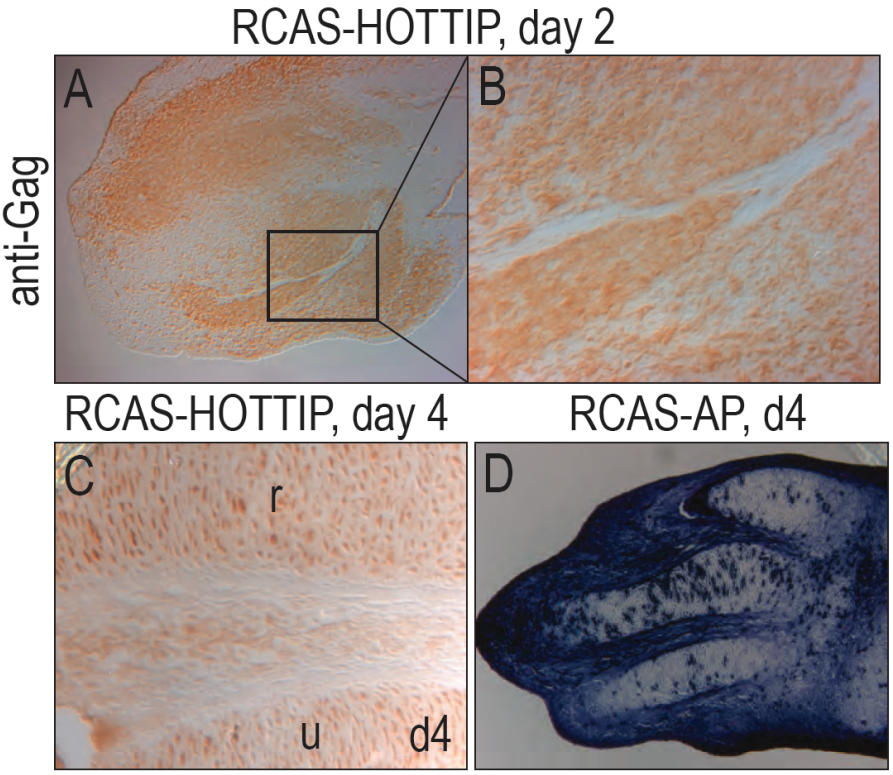


**Figure S4**. Efficient retroviral infection in developing chick limb buds. (A) Broad expression of the avian virus protein Gag in mesenchymal cells of chick forelimb 2 days after injection with RCAS-shHOTTIP. (B) Higher magnification of A showing detection of Gag protein in mesenchymal and muscle cells of the injected limb. (C) After 4 days of injection, Gag protein was detected in limb chondrocytes. (D) Alkaline phosphatase activities were detected in hindlimb injected with control RCAS-AP. r, radius, u, ulna.

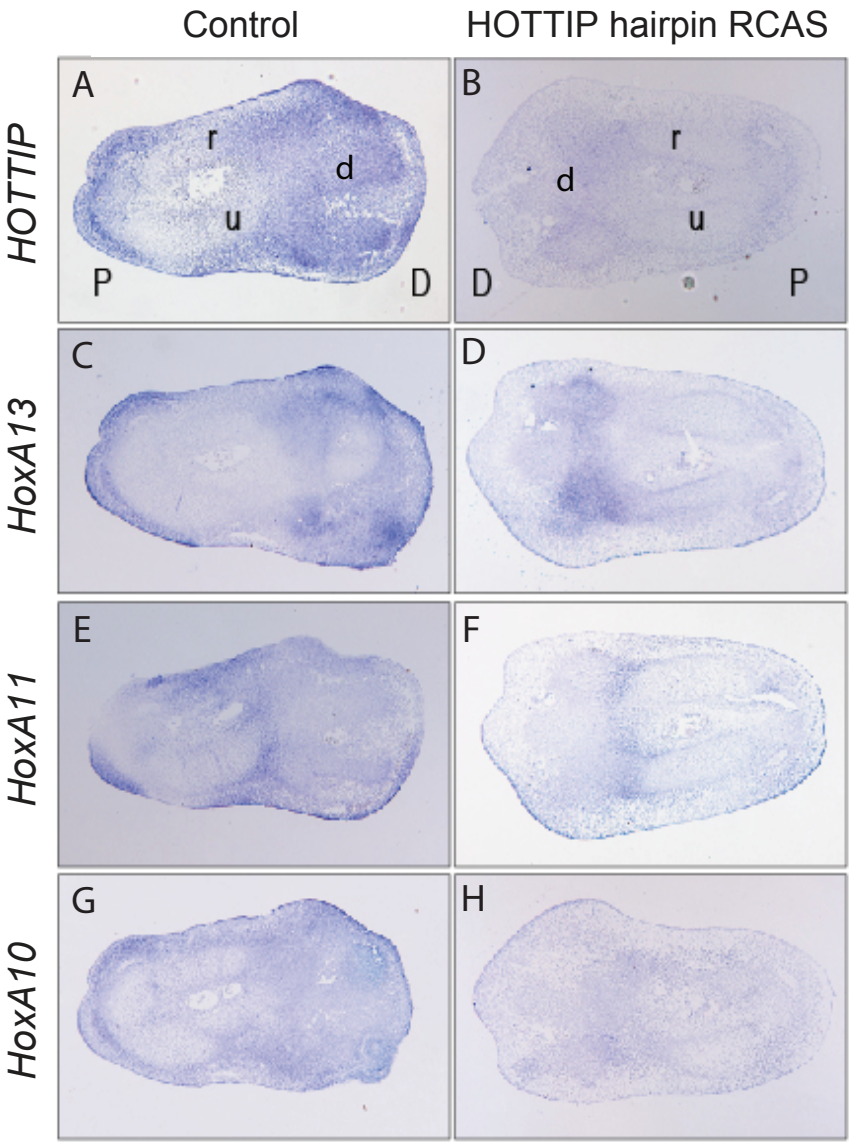


**Figure S5**. HOTTIP knockdown decreases expression of 5' *HoxA* genes in vivo. Replication competent avian virus (RCAS) expressing short hairpin RNA targeting HOTTIP was injected into chick limb buds at St. 17. After 4 days of incubation, embryos were harvested and prepared for sections and in situ hybridization. Contralateral limbs served as controls. Shown are forelimb zeugopod and autopod (i.e. elbow to fingertip). (A) *HOTTIP* expression in the limb bud is reduced (B) following over-expression of HOTTIP shRNA. In control limbs (C,E,G), *HoxA13*(C), *HoxA11* (E), and *HoxA10* (G) expression domains are strongest in distal, undifferentiated limb mesenchyme. In treated limbs (D,F,H) the expression domains of the *HoxA* genes are reduced in size and fewer transcripts are detectable. Abbreviations: r=radius (anterior side of limb); u=ulna; d= digit, D=distal tip of limb bud; P= proximal end .

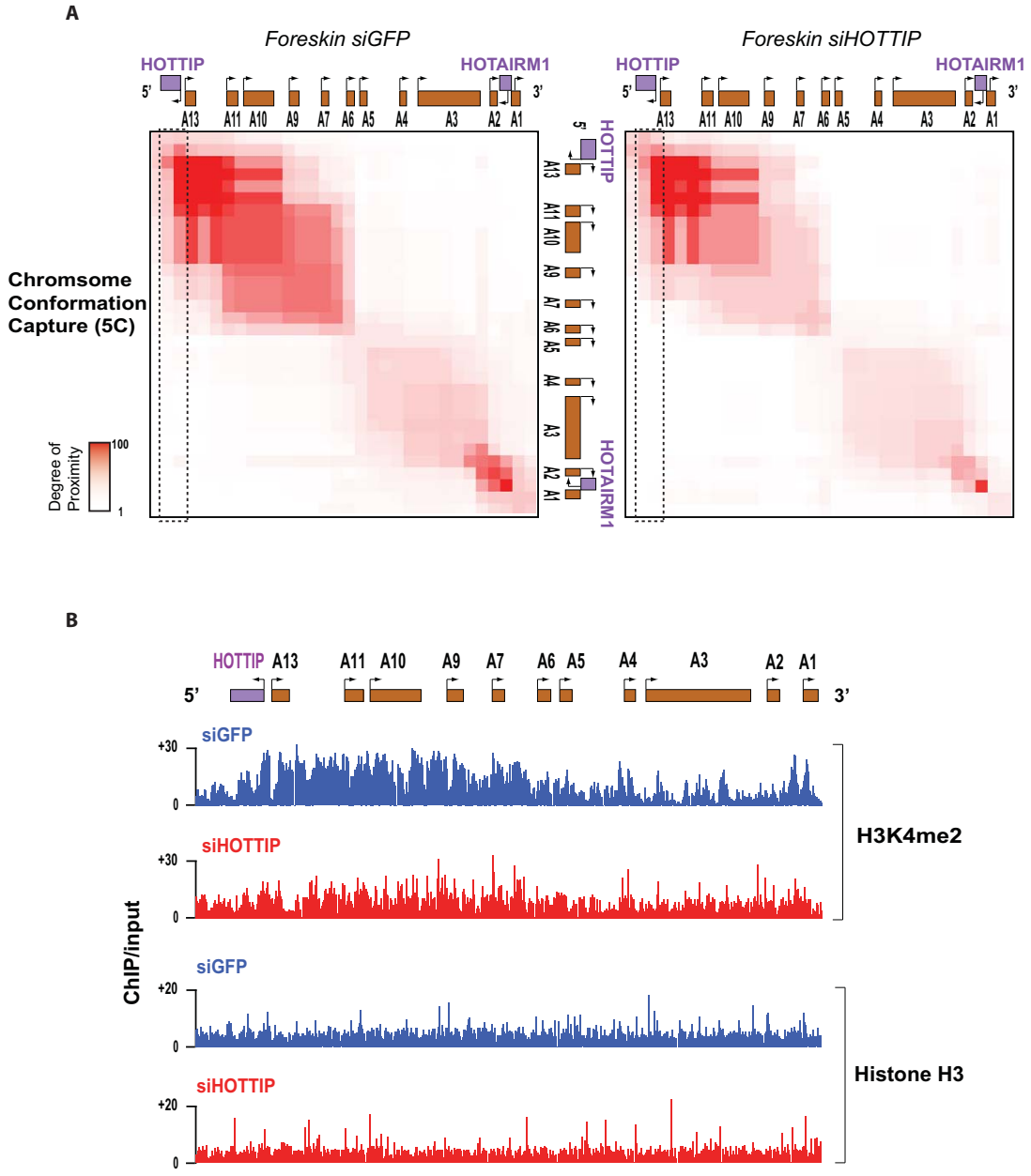


**Figure S6**. HOTTIP depletion causes little change to higher-order chromosome configuration. (A) Chromosome Conformation Capture (5C) analysis of foreskin fibroblasts treated with control siRNAs (siGFP) or siRNA targeting HOTTIP. Heatmap representations of 5C data (bin size 30 kb, step size 3 kb) across human *HOXA* are as in

Fig. 1A. The diagonal represents frequent cis interactions between regions located in proximity to each other in the HoxA locus. Long-range looping interactions are 5C signals that are away from the diagonal. Each pixel represents median interactions in a 30kb region; the intensity of pixel corresponds to the total number of reads. (B) Knockdown of HOTTIP broadly decreases H3K4me2 across 5' *HOXA* locus but does not change overall occupancy of histone H3. ChIP-chip data across ~100 kilobase *HOXA* locus are shown for foreskin fibroblasts with control (top) versus HOTTIP (bottom) knockdown. Genomic coordinate is on the X-axis; Y-axis depicts relative occupancy of H3K4me2 and pan histone H3 on a linear scale.

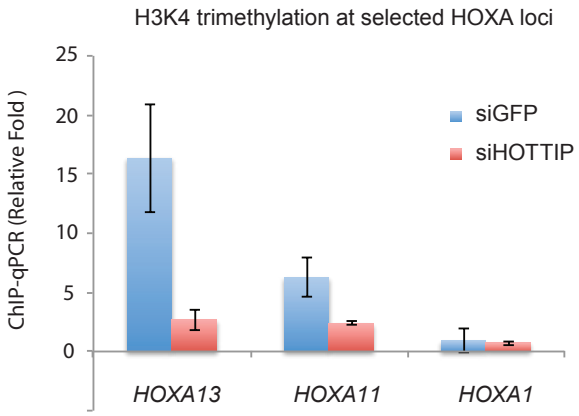


**Figure S7**. ChIP-qPCR validation of HOTTIP-dependence of H3K4me3 occupancy at distal *HOXA*. Chromatin-immunoprecipitation with H3K4me3 was performed on foreskin fibroblasts transfected with siRNA against GFP (siGFP) or HOTTIP (siHOTTIP), and the subsequent enrichment of distal (*HOXA13*, *HOXA11*) and proximal (*HOXA1*) *HOXA* genes were analyzed by quantitative PCR. Mean ± s.d. are shown.

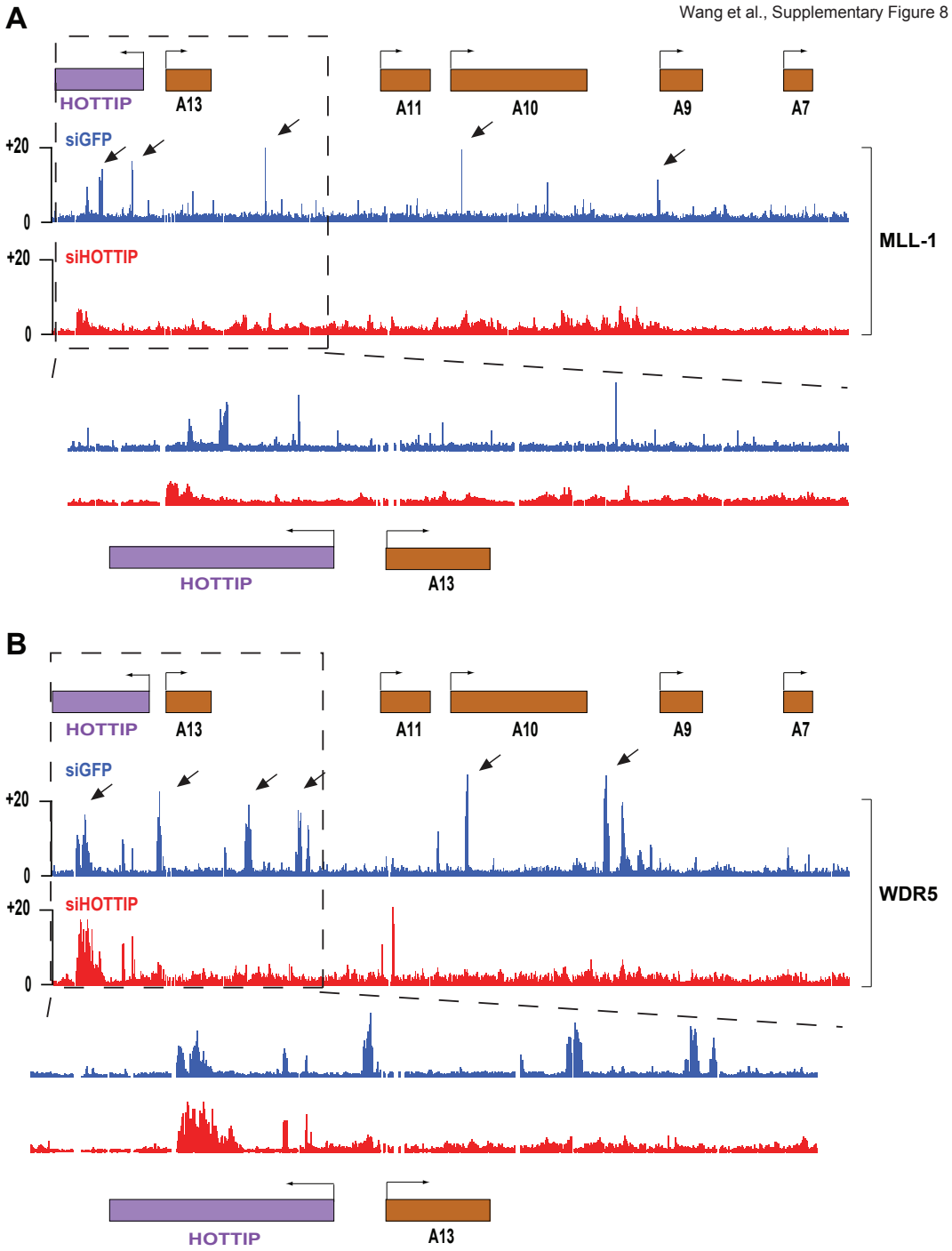


**Figure S8**. Zoom-in view of Fig. 3 highlighting HOTTIP dependence of MLL1 and WDR5 localization to *HOXA*. Knockdown of HOTTIP abrogates MLL1(A) and WDR5 (B) peaks across the 5' *HOXA* locus, and results in diffuse and less intense binding of MLL1 and WDR5 across the 5'*HOXA*. HOTTIP knockdown also led to increased accumulation of MLL1 and WDR5 on *HOTTIP* itself. Arrows highlight peaks of MLL1 and WDR5 occupancy.

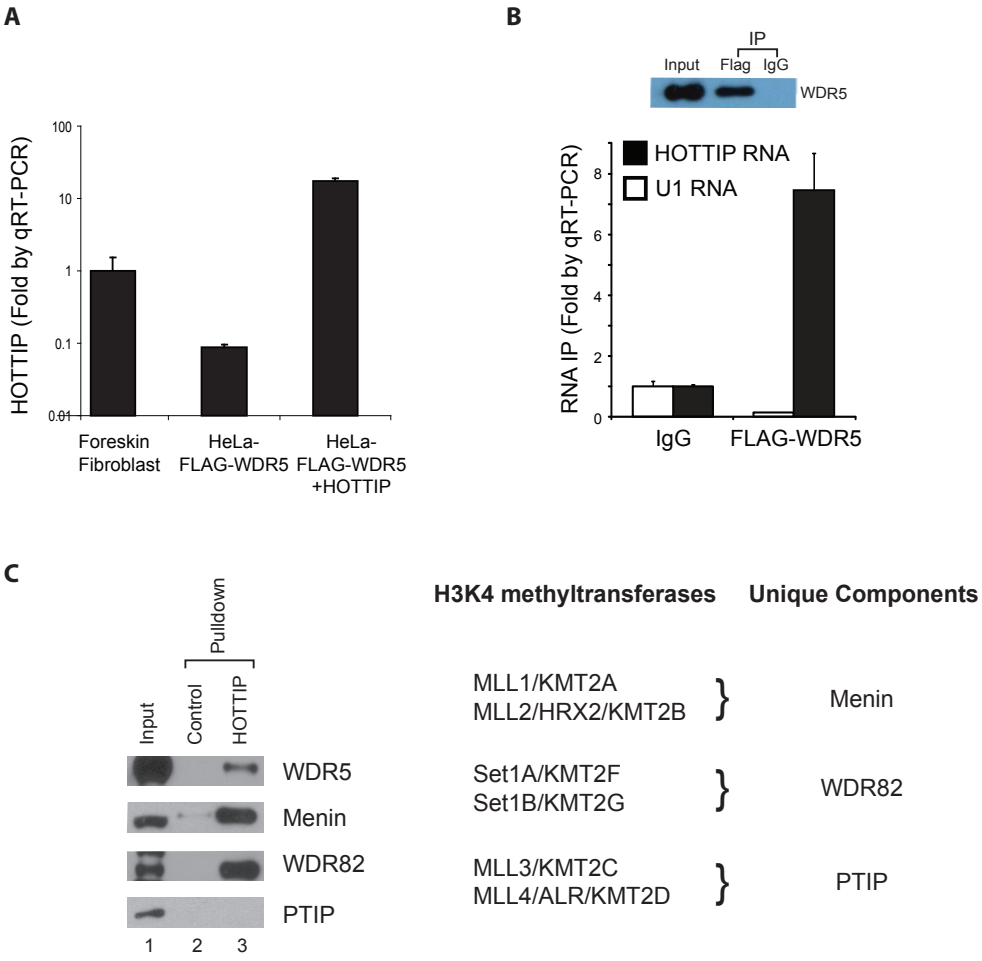


**Figure S9**. HOTTIP binds stably expressed FLAG-WDR5 in HeLa cells. (A) HOTTIP expression levels in primary foreskin fibroblasts, FLAG-WDR5 HeLa cells, and FLAG-WDR5 HeLa cells transduced with HOTTIP. Error bars represent mean ± s.d.. (B) HOTTIP binds specifically to WDR5 in cells. Top: IP of FLAG-WDR5 verified by WDR5 immunoblot. Bottom: Quantitation of RIP by qRT-PCR, normalized by the levels of RNA retrieved by IgG control. (C) RNA binding by H3K4 methylase complexes. Extract from from FLAG-WDR5 HeLa cells were passed over beads (control) or bead coupled to full-length HOTTIP RNA, extensively washed, and interrogated for retrieval of specific proteins by immunoblot. HOTTIP retrieved WDR5, Menin (unique to MLL1/MLL2 complexes), and WDR82 (unique to the Set1A/Set1B), but not PTIP (unique to MLL3/MLL4 complexes).

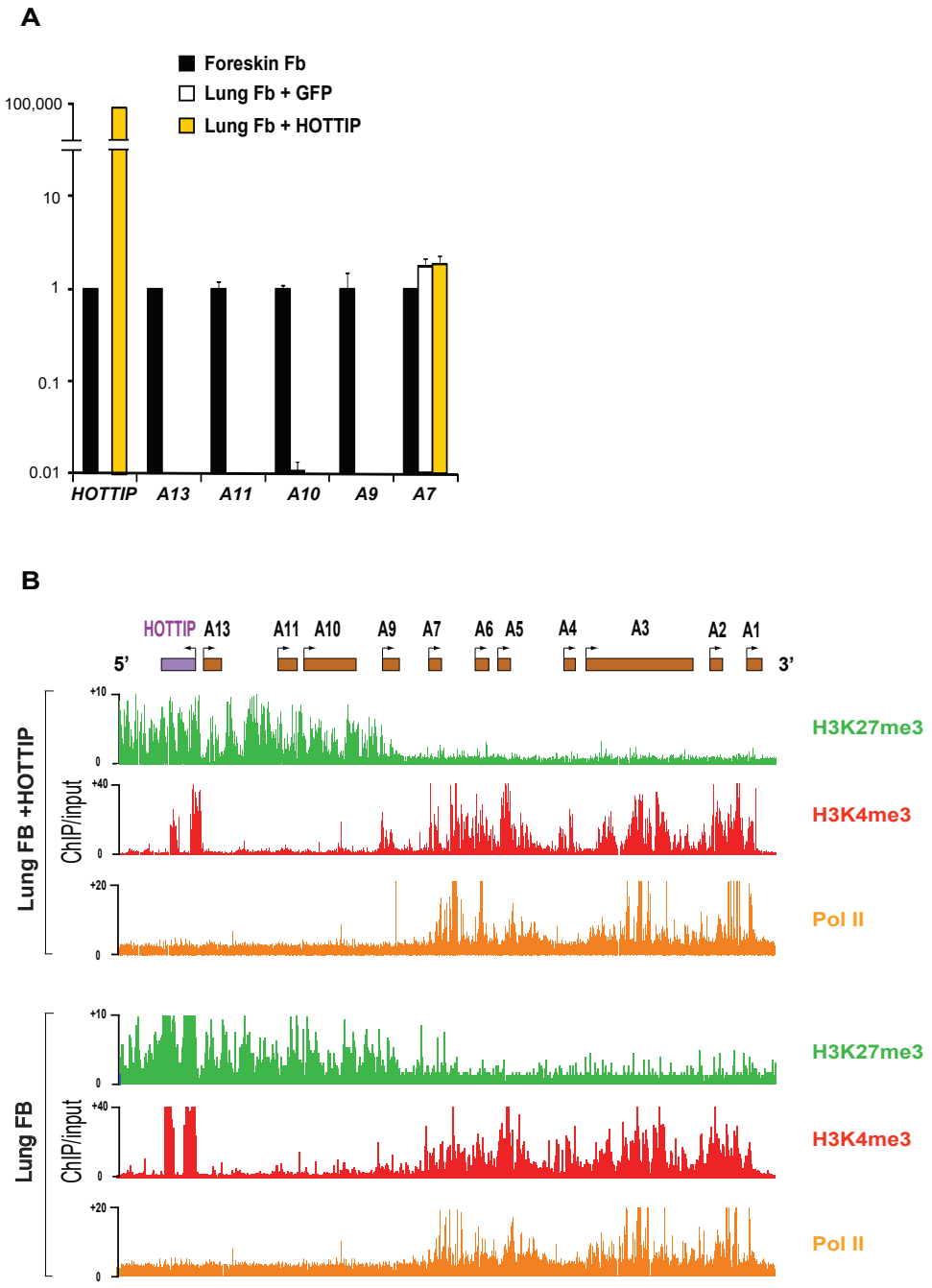


**Figure S10**. HOTTIP overexpression does not affect distal *HOXA* expression. (A) Ectopic overexpression of HOTTIP in lung fibroblasts does not activate 5'*HOXA* genes. (B) HOTTIP overexpression in lung fibroblasts do not change *HOXA* chromatin state. ChIP-chip data across ~100 kilobase *HOXA* locus are shown for lung fibroblasts overexpressing HOTTIP (top) compared those from regular lung fibroblasts (bottom). Genomic coordinate is on the X-axis; Y-axis depicts relative occupancy of H3K27me3, H3K4me3, and RNA polymerase II (Pol II) on a linear scale.

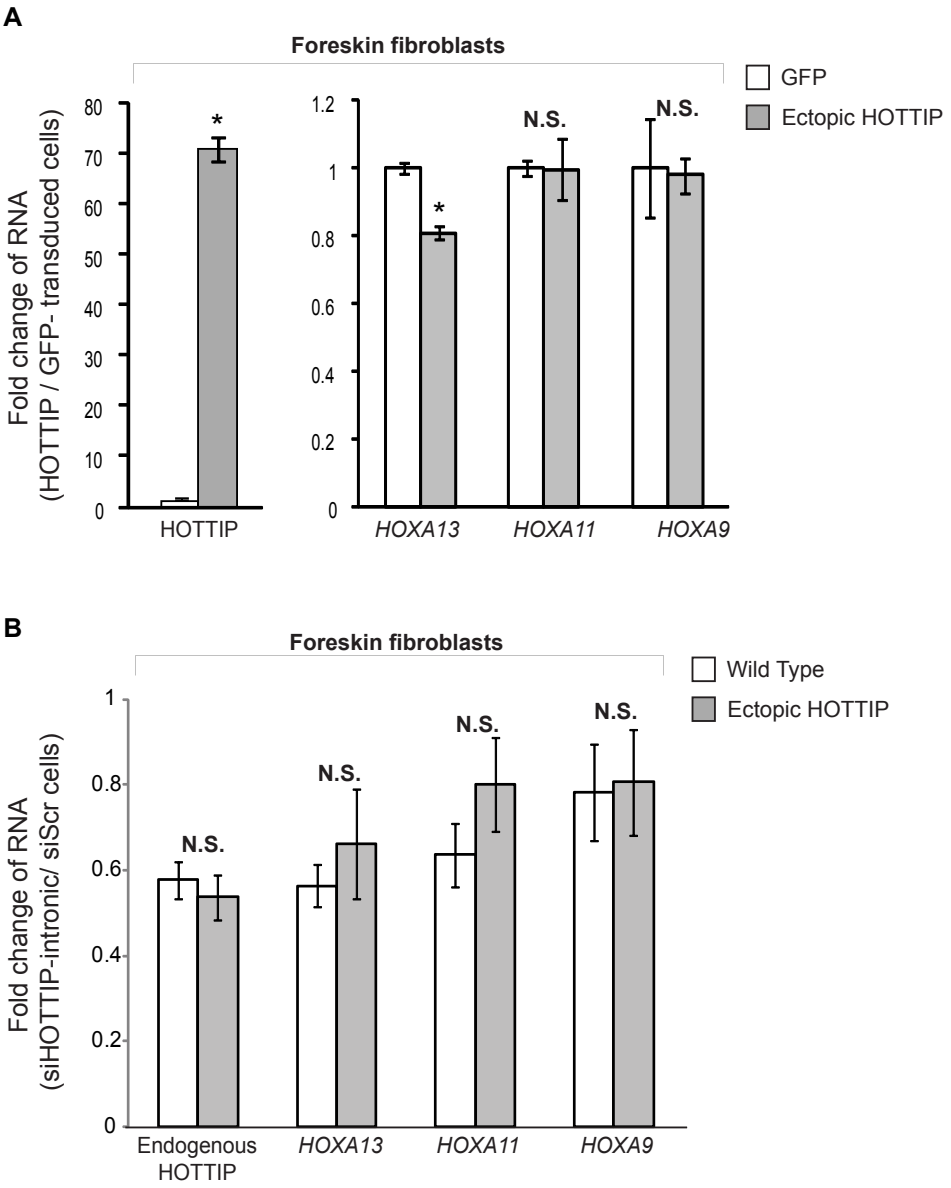


**Figure S11**. Ectopic HOTTIP expression does not activate 5'*HOXA* genes nor rescue the effects of depleting endogenous nascent HOTTIP. (A) HOTTIP overexpression in foreskin fibroblasts is unable to activate 5'*HOXA* genes, and has apparently dominant negative effect on *HOXA13* expression. GFP transduction served as negative control, which did not change HOTTIP level or 5' *HOXA* genes. (B) Knockdown of endogenous nascent HOTTIP was achieved by siRNAs targeting intronic regions in HOTTIP, leading to decreased expression of 5' *HOXA* genes. siRNAs targeting HOTTIP introns do not affect ectopic HOTTIP overexpression from cDNA (>100 fold in both siScr vs. siHOTTIP-intronic treated cells compared to wild type). Cells transduced with ectopic HOTTIP cDNA responded to endogenous HOTTIP depletion in the same manner, indicating that ectopic HOTTIP cannot rescue depletion of endogenous HOTTIP. Mean ± s.d. are shown. *, $p<0.05$, Student's *t*-test. N.S., not significantly different between control and ectopic HOTTIP overexpression.

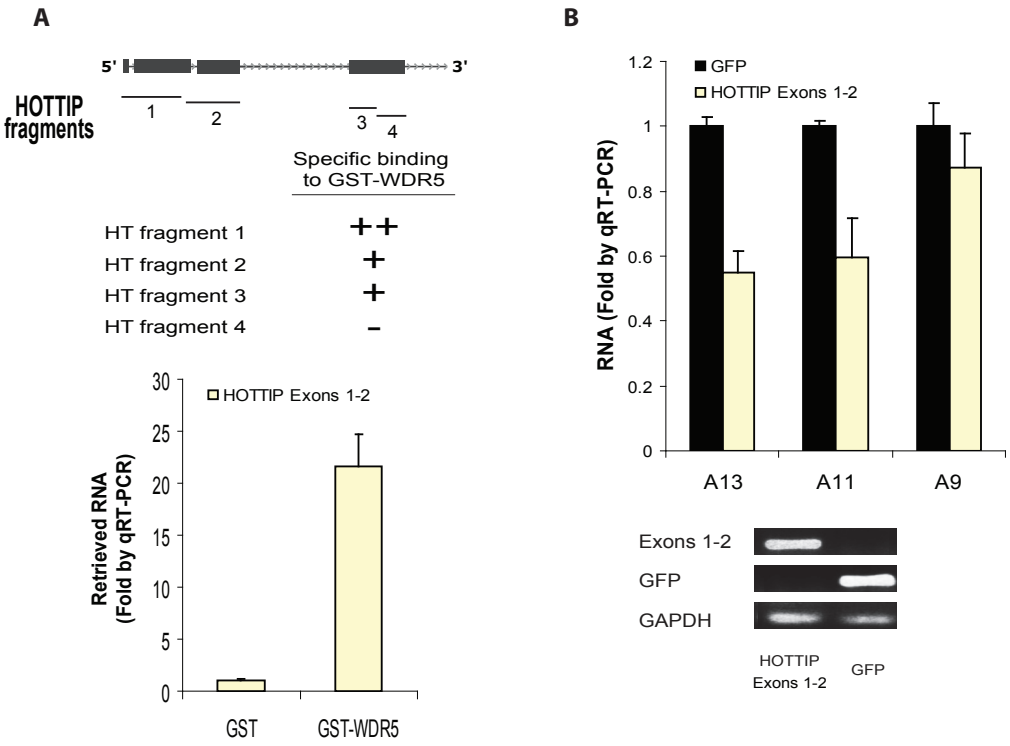


**Figure S12**. HOTTIP$^{Exons1-2}$ binds to WDR5 and acts in a dominant negative manner to inhibit 5' *HOXA* gene expression. (A) Schematic of HOTTIP fragments and their relative affinities in binding to GST-WDR5. Each fragment was in vitro transcribed and purified, and incubated with purified recombinant GST or GST-WDR5. Specific retrieval of RNA by GST-WDR5 was quantified by qRT-PCR. + indicates higher interaction with GST-WDR5 than GST. Notably, HOTTP exons 1-2 bound GST-WDR5 ~2 fold better than full length HOTTIP on a molar basis. Mean ±s.d. is shown. (B) Overexpression of HOTTIP$^{Exons1-2}$ in foreskin fibroblasts exerts a dominant negative effect, resulting in reduced 5' *HOXA* gene expression. Error bars represent s.d. from biologic duplicates. Bottom: Overexpression is confirmed by RT-PCR using primers specific for HOTTIP$^{Exons1-2}$ and GFP; GAPDH is included as a loading control.

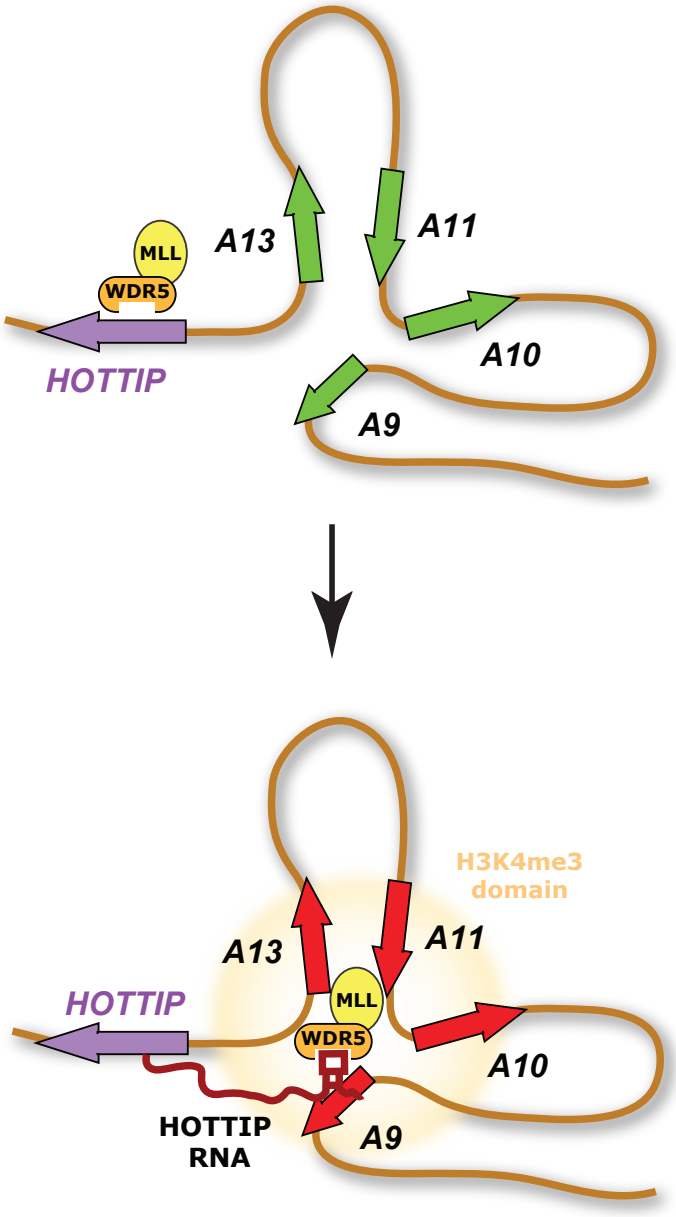


**Figure S13**. Model of HOTTIP action. *HOTTIP* is positioned near the active 5' HOXA genes via chromosomal looping. The top panel depicts the situation in distal cells when HOTTIP is depleted: the chromosome is looped to bring 5' *HOXA* genes together, but MLL1/WDR5 is not properly localized, nor is there H3K4me3 and gene transcription. Upon transcription (bottom panel), HOTTIP RNA binds to WDR5-MLL1 complex, and drives MLL1/WDR5 occupancy and H3K4 trimethylation of 5' *HOXA* genes. Because HOTTIP transcription is dependent on WDR5 and WDR5 occupancy is dependent on HOTTIP, this mutual interdependence creates a positive feedback loop that maintains the ON state of the 5' *HOXA* locus.

**Supplementary File Legends**

Supplementary File 1. 5C data. Binned data (median values of all interactions) from the 5C experiments—2 replicates of foreskin (HOX-FORESKIN-FB) and lung fibroblasts (HOX-LUNG-FB), and one set of knockdown experiments with control siRNA (HOX-siGFP-FORESKIN-FB) and siHOTTIP (HOX-siHOTTIP-FORESKIN-FB) on foreskin fibroblasts—used to generate the heatmaps in Figure 1A and Figure S6; Bin size=30kb, bin step size=30kb.

**Supplementary Table Legends**

**Supplementary Table 1.**

5C primers used for the interrogation of the HoxA locus (ENm010). In total, 17 reverse and 90 forward primers were designed in the 500Kb HoxA1 locus; hence, a total of 1530 *cis* interaction were interrogated in this region.

**Supplementary Table 2.**

Table of 5C experiment totals containing 15 columns. Library Name: 5C sample name, R1 & R2 denote biological replicate number; totalRead: total number of mapped 36bp Illumina GA2 paired end reads; totalInteractions: total number of unique 5C junctions (interactions); totalCis: total number of CIS (same interacting ENCODE regions) 5C interactions; totalCisPC: percentage of interactions in CIS; totalTrans: total number of TRANS (different interacting ENCODE regions) 5C interactions; totalTransPC: percentage of interactions in TRANS; hoxReads: total number of reads where at least one interactor mapped to the ENm010 (HOX) region; hoxPC: percentage of reads where at least one interactor mapped to the ENm010 (HOX) region; hoxCisReads: total number of ENm010 (HOX) region reads in CIS (ENm010:ENm010); hoxCisPC: percentage of ENm010 (HOX) region reads in CIS (ENm010:ENm010); hoxTransReads: total number of ENm010 (HOX) region reads in TRANS (ENm010:other region); hoxTransPC: percentage of ENm010 (HOX) region reads in TRANS (ENm010:other region); elseReads: total number of reads mapping to other included ENCODE regions; elsePC: percentage of reads mapping to other included ENCODE regions; 1976_HOX-LUNG-FB-R1 and 1977_HOX-FORESKIN-FB-R1 libraries contained ENm010 (HOX) and 1 other region (ENr313). 2156_HOX-LUNG-FB-R2, 2159_HOX-SIGFP-FS-R1,

2245_HOX-FORESKIN-FB-R2 and 2246_HOX-SINC13-FS-R1 libraries contained ENm010 (HOX) and 30 other regions (all ENCODE random regions - ENr).

**Supplementary Table 3.**

Sequences of quantitative PCR (qPCR) primers and siRNA against intronic HOTTIP (siIntronic 1 through 10). The siRNAs were combined and used as a pool in the nascent HOTTIP knockdown experiments shown in Fig. S11.

**References**


1 Chang, H. Y. *et al.* Diversity, topographic differentiation, and positional memory in human fibroblasts. *Proc Natl Acad Sci U S A* **99**, 12877-12882 (2002).

2 Chang, H. Y. *et al.* Gene expression signature of fibroblast serum response predicts human cancer progression: Similarities between tumors and wounds. *PLoS Biology* **2**, 206-214 (2004).

3 Bernstein, B. E. *et al.* Genomic maps and comparative analysis of histone modifications in human and mouse. *Cell* **120**, 169-181 (2005).

4 Rinn, J. L., Bondre, C., Gladstone, H. B., Brown, P. O. & Chang, H. Y. Anatomic demarcation by positional variation in fibroblast gene expression programs. *PLoS Genet* **2**, e119 (2006).

5 Rinn, J. L. *et al.* Functional demarcation of active and silent chromatin domains in human HOX loci by noncoding RNAs. *Cell* **129**, 1311-1323 (2007).

6 Rinn, J. L. *et al.* A dermal HOX transcriptional program regulates site-specific epidermal fate. *Genes Dev* **22**, 303-307 (2008).

7 Rinn, J. L. *et al.* A systems biology approach to anatomic diversity of skin. *J Invest Dermatol* **128**, 776-782 (2008).

8 Soshnikova, N. & Duboule, D. Epigenetic temporal control of mouse Hox genes in vivo. *Science* **324**, 1320-1323 (2009).

9 Wysocka, J. *et al.* WDR5 associates with histone H3 methylated at K4 and is essential for H3 K4 methylation and vertebrate development. *Cell* **121**, 859-872 (2005).

10 Dostie, J. *et al.* Chromosome Conformation Capture Carbon Copy (5C): a massively parallel solution for mapping interactions between genomic elements. *Genome Res* **16**, 1299-1309 (2006).

11 Lajoie, B. R., van Berkum, N. L., Sanyal, A. & Dekker, J. My5C: web tools for chromosome conformation capture studies. *Nat Methods* **6**, 690-691 (2009).

12 Harrow, J. *et al.* GENCODE: producing a reference annotation for ENCODE. *Genome Biol* **7 Suppl 1**, S4 1-9 (2006).

13 Birney, E. *et al.* Identification and analysis of functional elements in 1% of the human genome by the ENCODE pilot project. *Nature* **447**, 799-816 (2007).

14 Dostie, J. & Dekker, J. Mapping networks of physical interactions between genomic elements using 5C technology. *Nat Protoc* **2**, 988-1002 (2007).

15 Sasaki, Y. T., Sano, M., Kin, T., Asai, K. & Hirose, T. Coordinated expression of ncRNAs and HOX mRNAs in the human HOXA locus. *Biochem Biophys Res Commun* **357**, 724-730 (2007).

16 Raj, A., van den Bogaard, P., Rifkin, S. A., van Oudenaarden, A. & Tyagi, S. Imaging individual mRNA molecules using multiple singly labeled probes. *Nat Methods* **5**, 877-879 (2008).

17 Harpavat, S. & Cepko, C. L. RCAS-RNAi: a loss-of-function method for the developing chick retina. *BMC Dev Biol* **6**, 2 (2006).

18 Smith, D. B. & Johnson, K. S. Single-step purification of polypeptides expressed in Escherichia coli as fusions with glutathione S-transferase. *Gene* **67**, 31-40 (1988).

19 Dignam, J. D., Lebovitz, R. M. & Roeder, R. G. Accurate transcription initiation by RNA polymerase II in a soluble extract from isolated mammalian nuclei. *Nucleic Acids Res* **11**, 1475-1489 (1983).

20 Michlewski, G. & Caceres, J. F. RNase-assisted RNA chromatography. *Rna* **16**, 1673-1678 (2010).

21 Lan, F. *et al.* A histone H3 lysine 27 demethylase regulates animal posterior development. *Nature* **449**, 689-694 (2007).

22 Rosenbloom, K. R. *et al.* ENCODE whole-genome data in the UCSC Genome Browser. *Nucleic Acids Res* **38**, D620-625 (2010).